Research Article GU J Sci 36(3): 1200-1215 (2023) DOI: 10.35378/gujs.1116423

Gazi University

Journal of Science

http://dergipark.gov.tr/gujs

Lumbar Spinal Stenosis Analysis with Deep Learning Based Decision Support Systems

Sinan ALTUN*, Ahmet ALKAN

Avşar Campus – Depertment of Electrical and Electronics Engineering Kahramanmaras Sutcu Imam University, 46050, Kahramanmaras, Türkiye

Highlights

- In deep learning, segmentation has been increased by going deeper.
- The basis of a system to assist the difficult manual detection of spinal stenosis has emerged.
- An up-to-date resource has been created for those who will work on this subject.

Article Info

Received: 13 May 2022
Accepted: 04 Aug 2022

Keywords

Unet
Deep learning
Image processing
Lumbar spinal stenosis
Semantic segmentation

Abstract

Lumbar spinal stenosis (LSS) is a condition that affects the quality of life of the 3 vertebrae, the disc and the canal in the lower back. In this region, the nerves in the canal may be subjected to pressure for various reasons, and disease occurs. Surgical intervention is required to treat canal stenosis, and the exact location and size of the spinal stenosis is critical to the surgery. The UNet model, which is an example of this network, can be further deepened with various deep learning networks. In this study, it will be the basis for creating a system that helps in the diagnosis of spinal stenosis by using a deeper network. The ResUNET model using ResNet as the backbone achieved an average IoU of 0.987. This study demonstrated that expert decision support systems using MR images can be used in the diagnosis of LSS.

1. INTRODUCTION

The spine carries the body and allows the body to stand upright; It is a very important structure especially for our movements. The spine also includes the canal in the middle of the vertebrae, called the spinal canal (spinal canal), through which the spinal cord passes. The spinal cord in the lower back carries the nerves that give sensation and strength to the legs. In case of stenosis of the canal between the vertebrae; accordingly, the spinal cord and nerve roots passing through it are compressed. This is the most common cause of spinal stenosis [1].

Age progresses due to the loss of water from the discs between the vertebrae in the spine starts from contraction. In response to this situation, extra bone formation, i.e. calcification, is observed in the spine and lower waist joints. In addition, the yellow connective tissues connecting the vertebrae tend to thicken into the canal and the disc hangs into the canal. As a result of all these symptoms, the spinal stenosis to a certain extent. It is possible to say that the spinal stenosis is a disease that occurs as a result of the loss of the properties of the bones in the region where the spinal cord and nerves are located, and that puts pressure on the nerves. Due to this pressure, the spinal cord and nerves become unable to perform their normal functions [1, 2].

Patients with spinal stenosis typically lean forward when walking because of leg pain, numbness, and weakness, which may be accompanied by low back pain [2].

*Corresponding author, e-mail: s.altun@yaani.com

Different diagnostic methods are used to diagnose spinal stenosis from other diseases. The first step in diagnosing spinal stenosis is to obtain information about the patient's history and complaints. After obtaining data such as when the complaints started, where the pain is felt and other health problems, the patient is examined in the second stage. During the physical examination, a detailed neurological examination is performed by looking at the patient's strength, sensation and reflexes. As the third step, imaging tests are requested from the patient. X-ray is one of the most basic diagnostic tools in spinal stenosis. Spinal stenosis can be detected clearly with X-ray images. And also; In spinal stenosis, the canal diameter can be measured and the diagnosis can be made easily with MRI or tomography imaging [2]. Figure 1 shows the representation of normal and contracting spinal stenosis samples.

Figure 1. *Spinal stenosis*

Biomedical imaging (MR, CT..), the last step in the diagnosis of the disease, cannot be said to give a perfect result. We can count these shortcomings as image noises caused by the device and the movement of the patient during shooting, and the inability to clearly distinguish tissue transitions in the image with the naked eye. It is possible to remove image noise using computer software. Deep learning methods, which are the current version of machine learning techniques, achieve almost perfect results in image processing. In this way, tissues in biomedical images can be distinguished perfectly. Since it performs segmentation with high success in the techniques we used in our study, it may be useful in eliminating these deficiencies.

In our work using the dataset [3], the root canal space is called AAP (called the canal/space), which represents the area between the anterior and posterior. The width of the AAP depends on where in the spine the measurement is taken. Lumbar spinal stenosis can occur as stenosis of any part of the AAP and can be classified as central or lateral, depending on where it occurs. This condition is considered one of the main causes of chronic low back pain because the spinal canal and the lateral part of the AAP contain many nerve roots that travel from different parts of the spine to other parts. Body. Abnormal compression of any of them can put pressure on these roots and cause pain [4]. In Figure 2, there is the image of Disc 3 obtained with the Lumbar MR image of a patient with Lumbar Spine Stenosis, which is the cause of many diseases from chronic low back pain to foot numbness. Since it is important to detect intervertebral disc (Intervertebral Disc), nerve bundle (Thecal Sac), posterior part (Posterior Element) and canal/space AAP regions for the detection of spinal stenosis, these regions will be segmented.

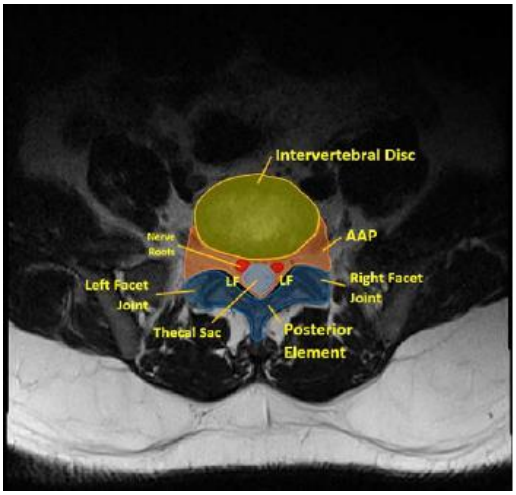

Figure 2. *Vertebrae, disc and canal*

In particular, spinal stenosis, which causes chronic low back pain, is caused by the canal in 3 vertebrae in the lumbar part [5]. Here; AAP segmentation of the intervertebral disc, posterior part (posterior element), nerve bundle (thecal sac) and cavity is a time-consuming process as well as requiring serious expertise.

In the study, the segmentation process will be done using UNet, one of the deep learning techniques. Commonly used techniques such as ResNet, Inception and VGG16 will be the backbone of the UNet model to go deeper in extracting segmentation features and increase performance. Figure 3 shows a block diagram of the proposed UNet model using ResNet, Inception, and VGG16 methods as the backbone.

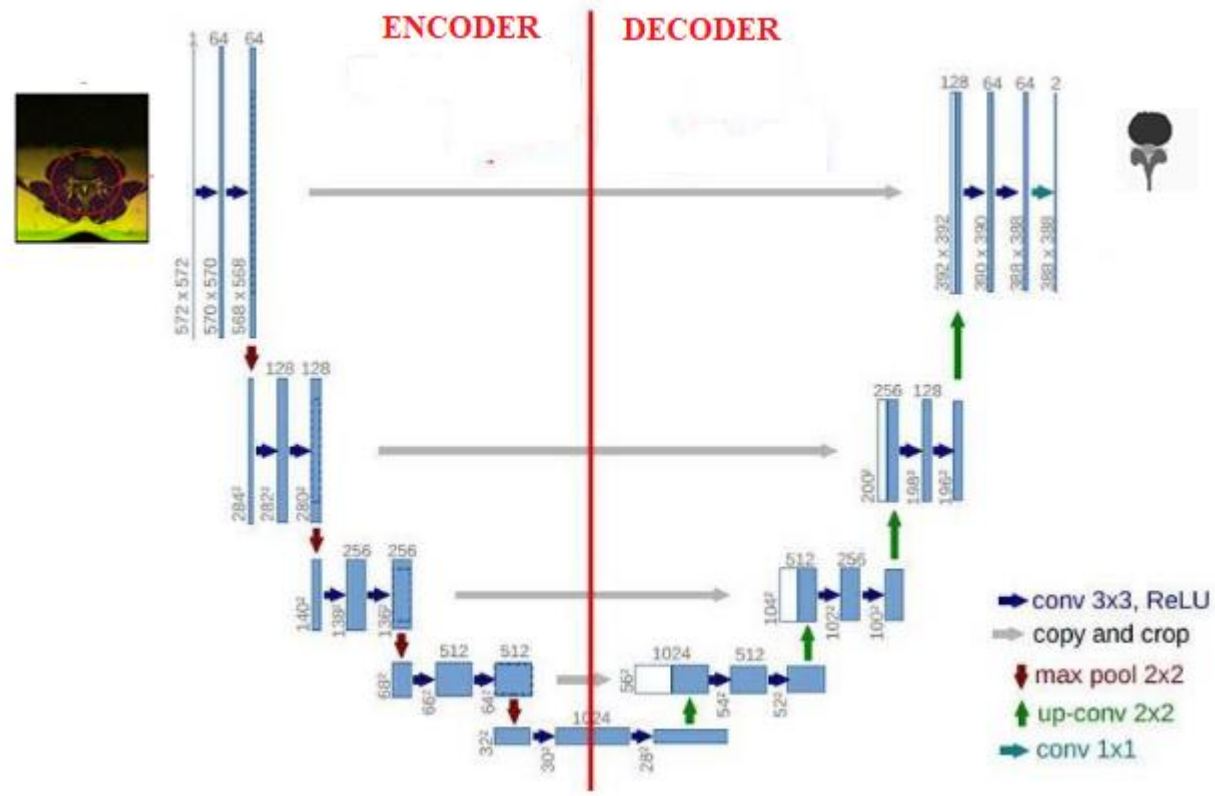

Figure 3. *Proposed UNet model*

In the first part, a summary of previous studies on the subject will be included. In the second part, information about the data set will be given. In the third part, information will be given about the U-Net model to be used in segmentation and ResNet, Inception and VGG16, which will form the backbone of this model. In the fourth chapter, the IoU (Intersection Over Union) values obtained from the experiments and what they mean will be shared. In the fifth chapter, the results of the study will be presented. In the last part, the results obtained will be evaluated and information will be given about how it will contribute to science and what kind of studies can be done in the future.

Back pain is a very common condition that can negatively impact life and is a major health problem. There are treatment options for this problem, starting with medication and then surgery. To this end, classical diagnostic methods rely on non-invasive imaging techniques such as tomography and MR imaging to assess intervertebral disc abnormalities (IVD). As a result of these analyses and clinical evaluations, the course of treatment is determined based on the experience of experts. They propose a new deep neural network architecture called "RIMNet", a region-to-image mapping network model that enables automatic and synchronized IVD recognition and segmentation of MRI images. The proposed model achieves a recognition accuracy of 94%. The results in the MICCAI IVD 2018 dataset are said to be validated by comparison with other methods [6].

Detecting axial disc herniation is difficult due to many difficulties, such as: B. The background is complex, the noise is loud, the image is blurry, and the task is arduous. The intervertebral disc is the small joint between the two vertebrae (L1-L2, L2-L3, L3-L4, L4-L5, and L5-S1). The most important task in computer-aided hernia diagnosis is the segmentation and localization of various intervertebral discs [7]. They stated that the goal of their work was to develop an automated system based on deep convolutional neural networks. Convolutional Neural Networks (CNNs) are of particular interest in this research. They decided to use an CNN based on the VGG16 architecture to detect disc herniation on MRI. Experiments were performed using a proprietary dataset from Sousse Sahloul University Hospital. The trained model achieved 94% accuracy, which represents a strong achievement in deploying state-of-the-art technology.

In this study on interverbal disc illnesses; They factor out that it's far an essential step forward in lots of scientific programs regarding segmentation, measurements, 3-D visualization, recording and computer-aided prognosis (CAD). selecting the right segmentation approach for a specific software is a difficult challenge. In maximum instances, a combination of several strategies can be necessary to attain the segmentation goal. there is a need to evaluate exceptional segmentation techniques using one-of-a-kind well-known protocols that help pick out methods for specific clinical programs. Disc degeneration is considered a totally not unusual spinal abnormality that reasons severe ache inside the again and legs and reasons many disruptions in humans' lives, and is now taken into consideration a prime purpose for patients to go to radiology clinics. in this study, unique techniques applied and the outcomes obtained for the analysis of vertebral and intervertebral disc disorder and degeneration are mentioned [8].

Spine clinicians have a laborious workload to perform comprehensive evaluations of multiple spinal structures on MRIs to detect abnormalities and investigate possible pathological factors. However, the study failed to achieve simultaneous semantic segmentation of intervertebral discs, vertebrae, and neural foramina due to the unusual triple challenges: 1) Multiple tasks, simultaneous semantic segmentation of multiple spinal structures is more difficult than individual tasks; 2) Multiple targets: average of 21 spinal structures per MRI, requires automated analysis, high diversity and variability; 3) Weak spatial correlations and subtle differences between normal and abnormal structures create dynamic complexity and uncertainty. First, Spine-GAN clearly solves the high diversity and variability of complex spine structures through an atrous convolution (i.e. hole convolution) autoencoder module, which can achieve semantic task-sensitive representation and preserve fine-grained structural information. Second, Spine-GAN dynamically models spatial pathological correlations between normally and abnormal structures, thanks to a specially designed long-short-term memory module [9].

An iterative sample segmentation approach using a fully convolutional neural network has been proposed to segment and label vertebrae one after another regardless of the number of visible vertebrae [10]. In this example, segmentation is enabled by combining the network with a memory component that holds information about the already segmented vertebrae. The mesh performs multiple tasks simultaneously, such as segmenting a vertebra, regressing its anatomical label, and predicting whether the vertebra is fully visible in the image; this allows vertebrae that are not fully visible to be excluded from further analysis. This method was evaluated with five different datasets, including multiple modalities (CT and MRI), various fields of view and coverage of different parts of the spine, and a particularly challenging series of low-dose chest CT scans. For vertebral segmentation, the DICE score is 94.9±2.1% with a mean absolute symmetrical surface distance of 0.2±10.1 mm. Anatomical identification has an accuracy of 93%, corresponding to a single case with mislabeled vertebrae.

2. MATERIAL

Magnetic Resonance (MR) images are also used in the diagnosis of Lumbar Spinal Stenosis [11, 12]. The data set used in our study consists of MR images.

The MR images to be used in the study are open access. Scientists who want to work in this field can obtain images from the link https://data.mendeley.com/datasets/k57fr854j2/2. The dataset consists of 515 MR images. Since spinal canal stenosis mostly occurs in the lumbar region, the axial view of the D3, D4 and

D5 vertebrae in the waist was taken. A total of 1545 MR images are included in the dataset. Data set was collected from different hospitals. All 1545 images are MR images of people with spinal stenosis.

The data set includes T1, T2-weighted MR images, as well as images obtained by combining T1 and T2. It is explained that the reason for processing T1 and T2 weighted images by combining them is that different features can be included in both sequences and segmentation can be done by extracting more useful information from the images obtained by combining them. All manual labeling of 1545 images was performed on T1-weighted MR, while experimental studies were performed on T1+T2 composite images.

In this study, 3 different experiments (ResUNet, Inception-UNet, VGG16UNet) will be performed on composite images. Figure 4 shows the image obtained by combining T1 and T2 MR images.

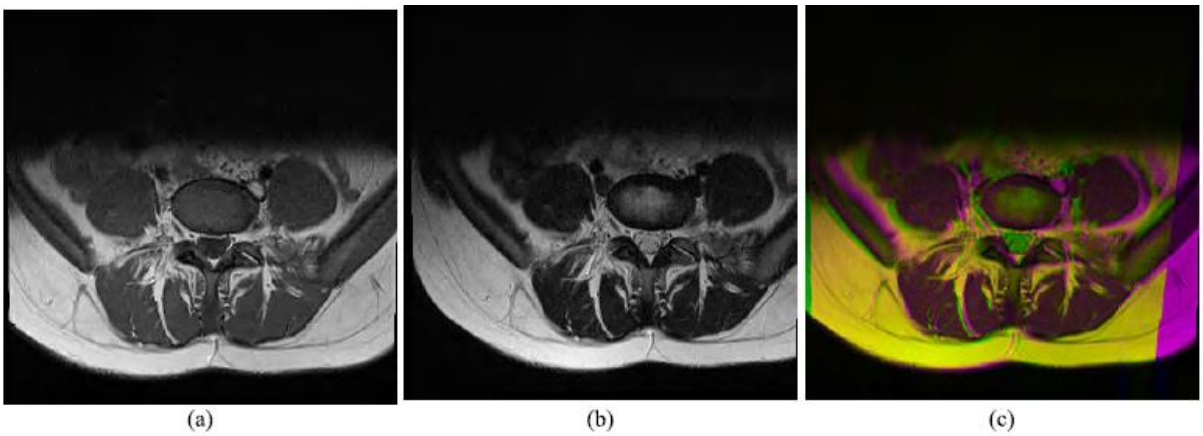

Figure 4. *a) T1 MR image, b) T2 MR image, c) T1+T2 MR image*

3. METHODS

3.1. Unet

The U-Net deep learning version [13] become evolved to perform scientific image segmentation. The model consists of two parts; the primary element is the encoder, which extracts features from the picture. The encoder includes a conventional convolutional layer and a max pooling layer. the second part is the component that makes use of the opposite transposed convolution, also referred to as the decoder. In truth, the encoder and decoder are programmed to be symmetrical to every other. U-internet is a totally convolutional stop-to-cease network containing only convolutional layers and no dense layers on the grounds that it is able to receive pics of any size [13] determine 5 suggests the structure of the classic UNet network. Figure 5 shows the U-Net deep learning architecture.

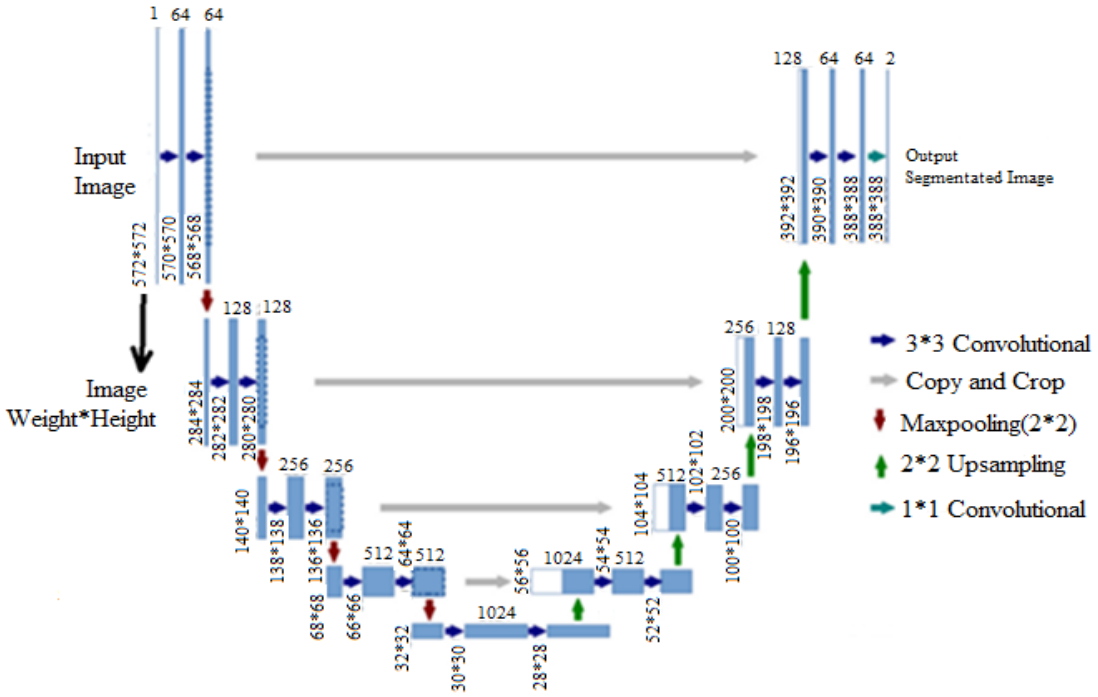

Figure 5. *UNet architecture*

Convolution

The color image consists of 3 channels, RGB, red, green and blue. For example, for a 512x512x3 image, the first value 512 represents the number of pixels in the width of the image, the second value 512 represents the number of pixels in length, and the third value 3 represents the number of channels. In fact, the computer treats this color image as three 512x512 matrices for three different color channels. This is performed on 2D matrices by image processing methods such as convolution and pooling [14, 15].

Blur, sharpen, edge detection, noise reduction, etc. operations allow us to extract feature maps from an image. When applied in image processing, a set of filters called "k" with dimension "f x f x number of channels" will be applied ("k" filters are also called Kernel or feature extractor). The output of the process is also a volume of size k. Output size "n_{out}" can be calculated according to Equation (1)

$$n_{out} = [(n_{in} + 2p - k)/s] + 1. \quad (1)$$

In Equation (1), "nin" denotes the input size of the image matrix, "p" the padding coefficient, "k" the size of the filter to be applied, and "s" the step coefficient to be applied.

We can express the images as 3 channels due to the combination of 3 different colors. When we translate a 1024x1024 image into computer language, a 1024x1024 matrix is obtained. A total of 3 matrices of this size within the 3 colors of the image are translated into computer language and the process is performed. In Figure 6, a 7x7x3 3-channel image matrix is shown as x[:,:,1], x[:,:,2] and x[:, : ,3]. Two filter matrices of 3x3x3 size applied to the image matrix are also included in Figure 6 as w[:,:,1], w[:,:,2] and w[:,:,3]. Here, “p=0” padding value is taken as “0”, “s=2” padding is taken as “2”. When calculated according to Equation (1), a 3x3 sized output matrix was obtained as a result of the applied process. Since 2 filters are applied, the number of channels has decreased to 1.

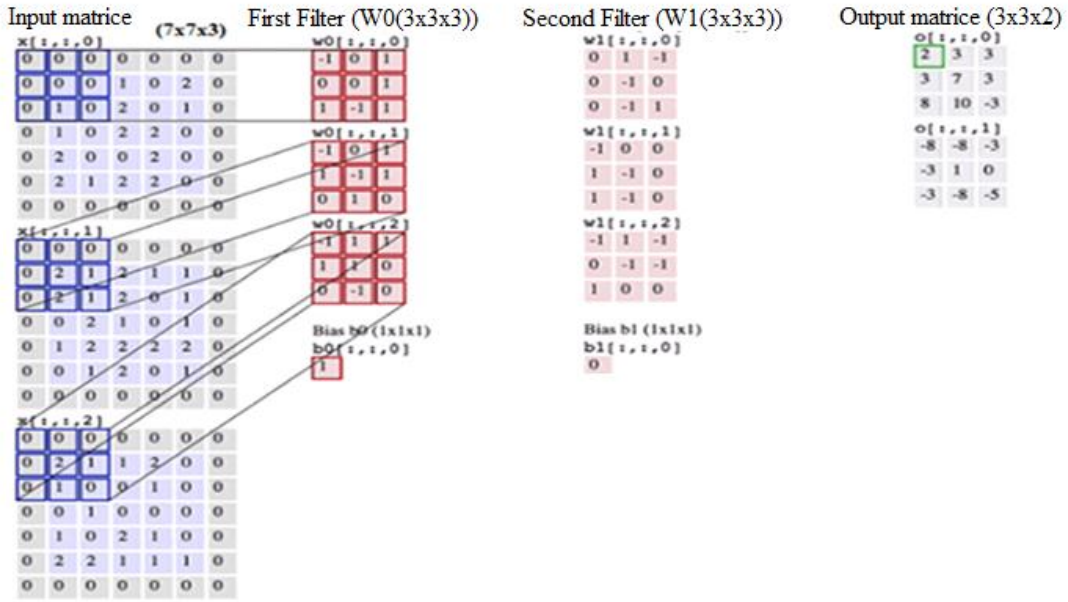

Figure 6*. Example matrix of convolution operation*

It is possible for the UNet model to use ResNet, Inception and VGG16 deep learning methods as a backbone. These models take place in the encoder part of the UNet model and can give detailed information about which class the pixels belong to. In this study, experiments will be carried out by combining these models with UNet.

Encoder

U-Net architecture takes its name from its shape, as seen in Figure 5. The coding part forms the left side of the U shape. When the convolution operation is repeatedly applied to extract features from the image, the image matrix decreases in size and increases in depth. As the mesh evolves, this shrinking size and increasing depth allows deeper filters to focus on a wider area. However, the number of channels/depth (number of filters used) increases gradually, which helps to extract more complex features from the image. Through the encoder, the model can better understand the content in the image [16].

Decoder

As can be seen in Figure 5, the right side of the UNet model is called the decoder. The decoder is performed using the transposed convolution method [16]. While there is a multiple of one in the convolution operation, it is the other way around in the decoding operation. An example of deconvolution of a 2x2 input image matrix with {2,1;4,4} values is shown in Figure 7. Here, in the Encoder section, it is explained how to expand the extracted pixel values.

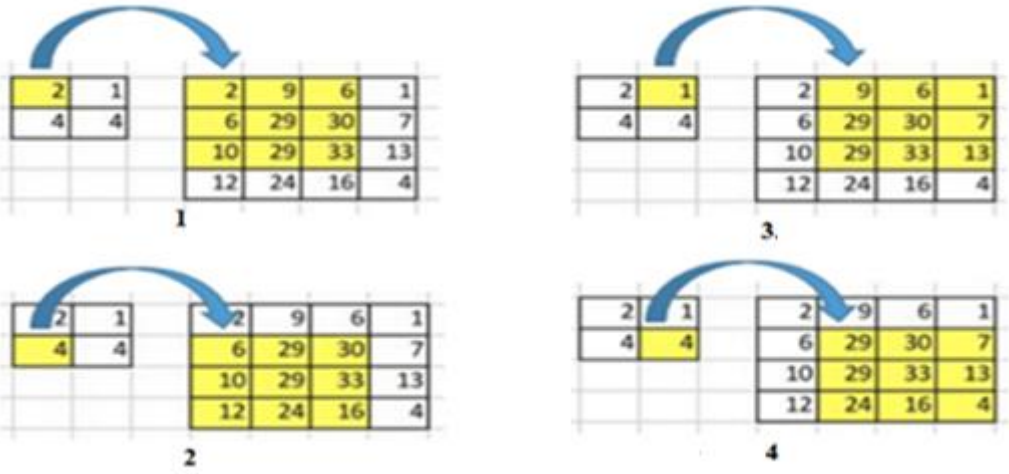

Figure 7*. Decoder/deconvolution*

3.2. ResNET

Networks can be deeper to extract more useful information from images. This brings with it some problems. As the network gets deeper, the number of parameters will be too large and computational difficulties will arise. In addition, the weights will gradually approach 0, and information will become undetectable from the image. It can be said that ResNet solves this problem in a simple way. It solves this problem of deep networks with a method called skipping connections. In Figure 8, the input goes to the output without going through the convolution layers, which are the weight layers [17, 18].

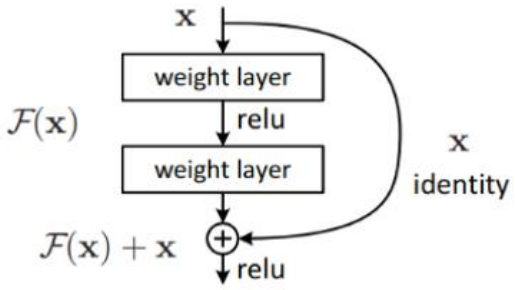

Figure 8*. Residual block*

Thanks to the jump, the output will be H(x), as can be seen in Equation (2)

$$H(x) = F(x) + x. \tag{2}$$

If F(x) is “0” in Equation (2), the output will be “x” and this is called Residual block identification.

If F(x) is not “0”, it is called a convolution block. As it is known, the dimensions must be the same in order to perform the convolution operation. Therefore, as can be seen in Equation (3), "x" is multiplied by a weight of "Ws" [17]

$$H(x) = F(x) + Ws * x. \tag{3}$$

3.3. InceptionNet

Created by Google, GoogLeNet increases depth while reducing network parameters. This allows LeNet to overlap with the network structure. Since the core of the LeNet network is the Inception network structure, it is possible to call the LeNet network the Inception network [19].

The initial module typically includes three different sizes of convolution and a maximum pooling. For the output of the previous layer, the channel is summed after the convolution process and then non-linear fusion is performed. In this way, the network's expression and adaptability to different scales can be improved and over-fitting can be prevented. Figure 9 shows the Inception network structure [19, 20].

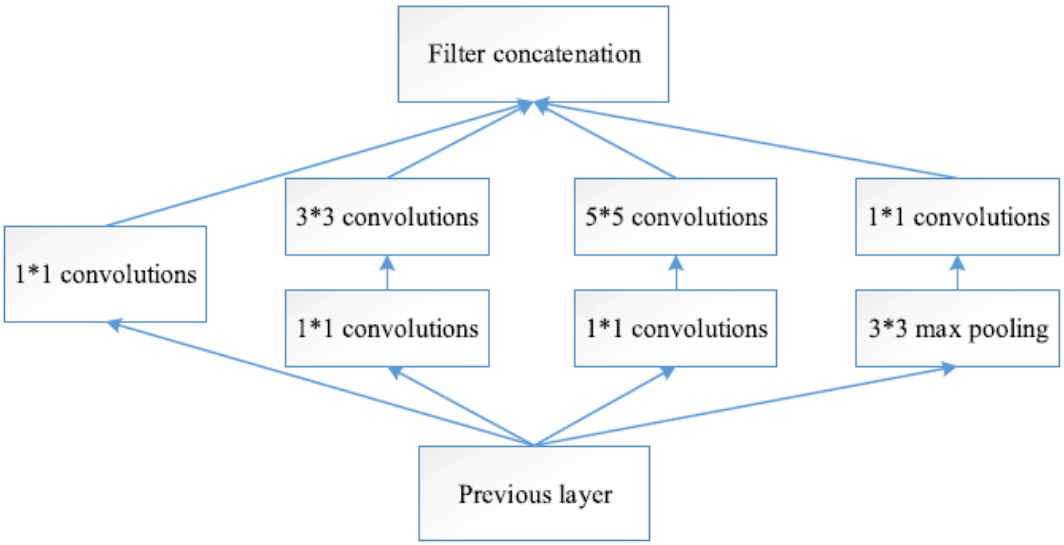

Figure 9. *Inception network structure (adapted from [19])*

3.4. VGG16

Actually VGG16 is a simple network model. The most important distinction from other models is the use of 2 or 3 convolution layers. In the full link layer, a feature vector with 7x7x512=4096 neurons is obtained. The 1000 class softmax performance is calculated on the two full link layer outputs. Calculation is made with approximately 138 million parameters. As in other models, while the height and width dimensions of the matrices decrease from the image input to the end, the number of channels increases [21].

Integrating VGG16 into the UNet model is easy. VGG16's calculation with high parameters allows it to go deeper on the image and extract detailed features. In fact, the ResNet and Incepiton models go even deeper. As with classical machine learning models, not every model is suitable for every data set. The structure of the VGG16 network is simply shown in Figure 10 [22].

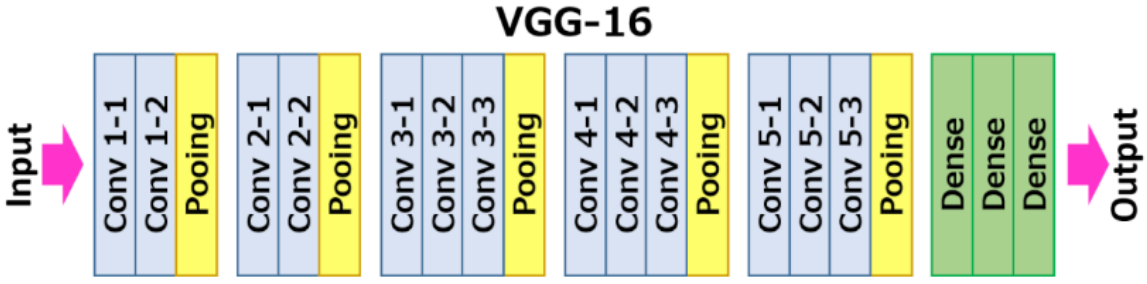

Figure 10*. VGG16 network structure*

3.5. Intersection over Union (IoU)

It will not be enough to give the success of image segmentation with accuracy alone. This is because UNet performs the calculation on each pixel individually. Therefore, it is necessary to evaluate which class it belongs to at the pixel level. This is where the Intersection Over Union (IoU) metric comes in. In order to understand this metric correctly, it is necessary to know the Ground Truth expression first. It refers to the value that should be included in the Ground Truth test dataset. In other words, it is the label value that the model you train should extract from the image in the test data. It is also called the IoU Jaccard index [23, 24].

In Figure 11, the area where the A and B images overlap is shown in red. The whole area ratio of this red area is expressed in IoU.

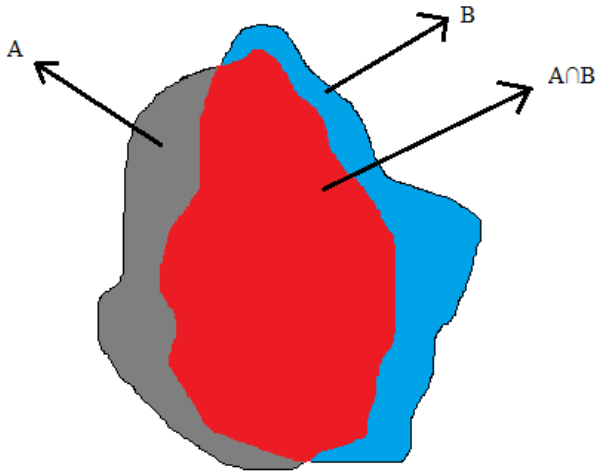

Figure 11. *Intersection over Union metric*

4. CONCLUCION

1545, T1+T2 MR images were examined with the ResUNet, Inception+UNet, and VGG16UNet models to find the model with the best segmentation. 1390 images were used for training and 155 images were used for testing. Although the experiments were performed with different epochs and hyper parameters, the best performance was obtained for the 3 models with the hyper parameters in Table 1. In order to find the most ideal hyper parameters in the study, the others except Epoch, Optimizer, Loss Function and Training/Test were tried as follows:

- Learning Rate: 0.1, 0.01, 0.001, 0.0001
- Batch Size: 0, 2, 4, 6, 8, 10

Table 1*. Hyperparameter values used in the experiments*

Hyperparameter Name:	Value:
Epoch	200
Learning Rate	0,0001
Batch Size	8
Optimizer	Adam
Loss Function	categorical_crossentropy
Training/Test	90/10

The experimental studies are summarized in Figure 12. The (a) ResUNet, (b) Inception+UNet, and (c) VGG16UNet models graphically represent the losses and IoU power values obtained on the 1545 images

in the MR data set. As can be seen from the graphs, VGG16UNet failed. Although Inception+UNet achieved serious success, ResUNet was the most successful model for this dataset.

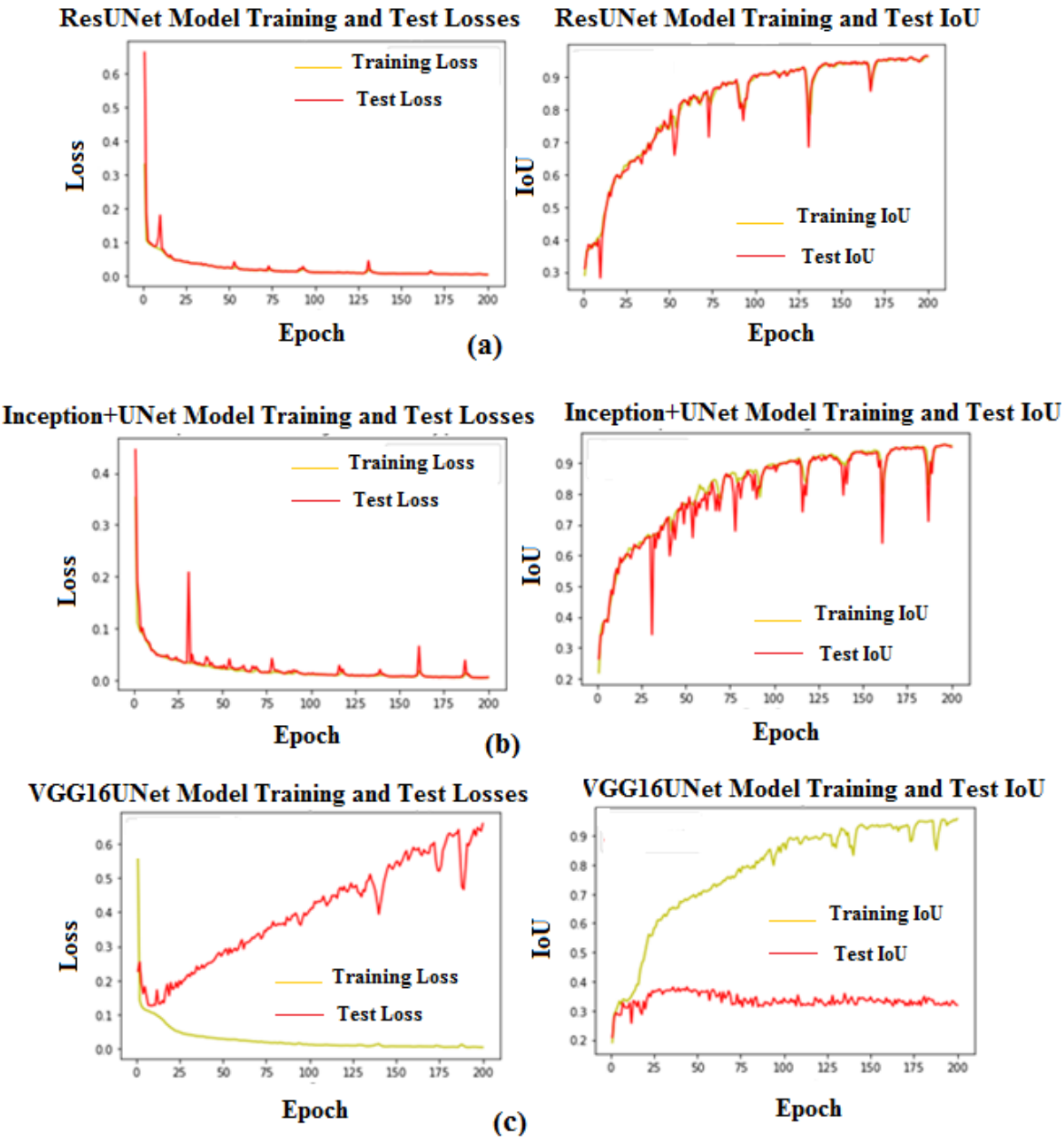

Figure 12. *a) ResUnet loss and IoU graph, b) Inception+UNet loss and IoU graph, c) VGG16UNet loss and IoU graph*

The segmentations obtained from some test images are shown in Figure 13. As can be seen in Figure 13(c), VGG16UNet was unable to fully segment any partition. In a), the success of the ResUNet model can be clearly seen.

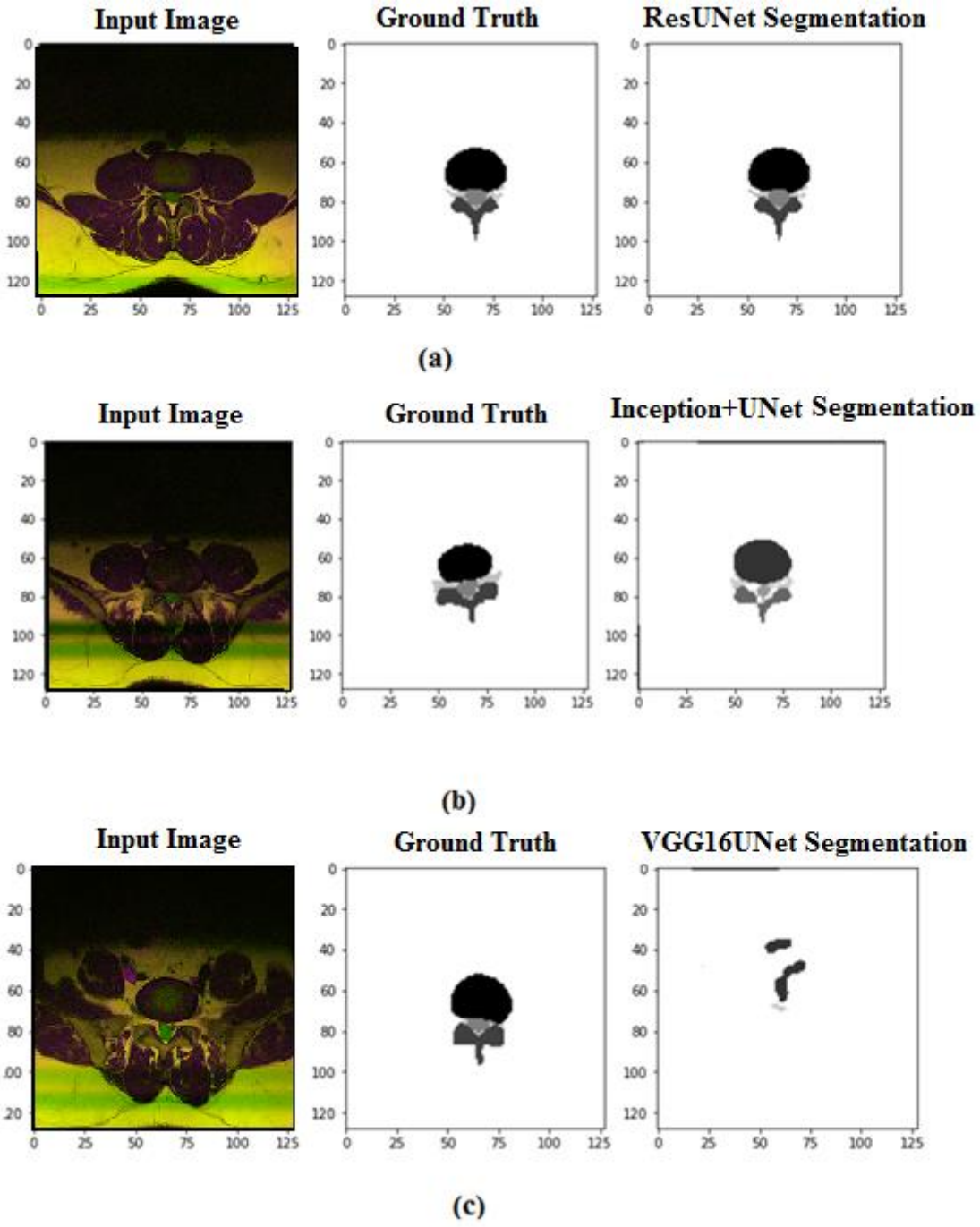

Figure 13. *a) ResUNet segmentation, b) Inception+UNet segmentation, c) VGG16UNet segmentation*

Spinal stenosis is a serious condition that, from chronic low back pain to numbness in the feet, limits the quality of life and causes sufferers to be unable to participate in working life. In this disease, which occurs mainly in the lumbar region, 3 vertebrae, the disc and the canal in the waist should be well segmented. In this study, 1545 MR images were used.

Experimental studies were performed with 3 different models for this dataset and the ResUNet model was proposed. Its high segmentation success is promising for the expert decision support system.

Table 2 shows both the IoU performance of the 3 models and the IoU performance of the previous study for this dataset. As can be seen in Table 2, ResUNet achieved the highest IoU for all classes. In addition,

Table 2 shows that the Inception+UNet model does not perform poorly compared to the study. Disc, posterior element, thecal sac, and AAP are important for correct segmentation here. In terms of segmentation of these classes, the Inception-UNet model is also very close to the previous study.

Table 2. *Model IoU success comparison*

Label/Class	[5] IoU of previous work	**ResUNet IoU**	Inception+UNet IoU	VGG16-UNet IoU
Unregistered	0,21	**0,998**	0,57	0,22
Intervertebral Disc	0,92	**0,999**	0,78	0,86
Posterior Element	0,78	**0,997**	0,71	0,59
Thecal Sac	0,85	**0,982**	0,8	0,16
AAP	0,53	**0,952**	0,56	0,13
Other	0,98	**0,999**	0,9	0,96

The literature was thoroughly reviewed and articles were found that directly segmented for LSS disease. The performance comparison, including the current article that performed segmentation of the lumbar disc near the study, is shown in Table 3. As shown in Table 3, the proposed model was the most successful result among the current publications.

Table 3. *Literature success comparison*

Authors:	**Name:**	**Journal:**	**Year:**	**Successes:**
Al-Kafri et al.[5]	Segmentation of Lumbar Spine MRI Images for Stenosis Detection Using Patch-Based Pixel Classification Neural Network	IEEE Congress on Evolutionary Computation	2018	mean IoU:0.72
Van der Graaf et al. [25]	Segmentation of vertebrae and intervertebral discs in lumbar spine MR images with iterative instance segmentation	Medical Imaging 2022: Image Processing	2022	mean Dice score of 93 % ± 2 % for vertebra segmentation and 86 % ± 7 % for IVD segmentation.
Silvestor et al. [26]	Efficient segmentation of lumbar intervertebral disc from MR images	IET Image Processing	2020	dice similarity index of 92.4%
Cheng et al. [27]	Automatic Segmentation of Specific Intervertebral Discs through a Two-Stage MultiResUNet Model	J Clin Med.	2021	segmentation accuracy is increased to about 94%
Proposed Method:	**Lumbar Spinal Stenosis Analysis with Deep Learning Based Decision Support Systems**	GU J Sci		Mean IoU: 0.98

5. DISCUSSION

Expert decision support systems are now being explored in the field of medicine. In particular, the scope of deep learning methods has reached unlimited dimensions. It is not possible for doctors to introduce health with practices that are as local and integrated as it is used for the practices of specialists because they are insufficient for this purpose. The day with scientists in this field is growing, in the hope that those who are clothed in the expert decision support system will graduate, live a quality life and educate schools.

In this study, a model for segmentation of the nerves, cavity, and disc was proposed, which is the preferred choice of the lumbar canal. ResUNet's reference model can achieve serious success for the current data set. Of course, these systems are not decision makers, but the decision is up to the expert. Although the model is promising, it needs to be tested on datasets obtained from much larger and different regions to obtain a better system.

Studies are being conducted on expert decision support systems to help identify lumbar canals with progressive sagittal MR images. Sagittal, axial and frontal MR imaging is used for 3-dimensional segmentation of canals, nerves and areas.

CONFLICTS OF INTEREST

No conflict of interest was declared by the authors.

ACKNOWLEDGEMENET

This study was funded by the THE SCIENTIFIC AND TECHNOLOGICAL RESEARCH COUNCIL OF TURKEY (TUBITAK (Project no: 122E042)) project entitled Lumbar Spinal Narrow Channel Analysis with Deep Learning Based Decision Support Systems.

REFERENCES

[1] Kiliçaslan, M.F., Nabi, V., Yardibi, F., Tokgöz, M.A., Köse, Z., "Research Tendency in Lumbar Spinal Stenosis over the Past Decade: A Bibliometric Analysis", World Neurosurgery, 149: 71–84, (2021).

[2] Seçen, A.E., Yiğitkanlı, K., "Lomber Dar Kanal; Patofizyoloji ve Doğal Seyir", Türk Nöroşirürji Dergisi, 28(2): 216 – 220, (2018)

[3] Natalia, F., Meidia, H., Afriliana, N., Al-Kafri, A.S., Sudirman, S., Simpson, A., Sophian, A., Al-Jumaily, M., Al-Rashdan, W., Bashtawi, M., "Development of Ground Truth Data for Automatic Lumbar Spine MRI Image Segmentation", 2018 IEEE 20th International Conference on High Performance Computing and Communications; IEEE 16th International Conference on Smart City; IEEE 4th International Conference on Data Science and Systems (HPCC/SmartCity/DSS). Published, 1449-1454, (2018).

[4] Al-Kafri, A.S., Sudirman, S., Hussain, A., Al-Jumeily, D., Natalia, F., Meidia, H., Afriliana, N., Al-Rashdan, W., Bashtawi, M., Al-Jumaily, M., "Boundary Delineation of MRI Images for Lumbar Spinal Stenosis Detection Through Semantic Segmentation Using Deep Neural Networks", IEEE Access, 7: 43487–43501, (2019).

[5] Al Kafri, A.S., Sudirman, S., Hussain, A.J., Al-Jumeily, D., Fergus, P., Natalia, F., Meidia, H., Afriliana, N., Sophian, A., Al-Jumaily, M., Al-Rashdan, W., Bashtawi, M., "Segmentation of Lumbar Spine MRI Images for Stenosis Detection Using Patch-Based Pixel Classification Neural Network", 2018 IEEE Congress on Evolutionary Computation (CEC), 1-8, (2018).

[6] Das, P., Pal, C., Acharyya, A., Chakrabarti, A., Basu, S., "Deep neural network for automated simultaneous intervertebral disc (IVDs) identification and segmentation of multi-modal MR images", Computer Methods and Programs in Biomedicine, 205, 106074, (2021).

[7] Mbarki, W., Bouchouicha, M., Frizzi, S., Tshibasu, F., Farhat, L.B., Sayadi, M., "Lumbar spine discs classification based on deep convolutional neural networks using axial view MRI", Interdisciplinary Neurosurgery, 22, 100837, (2020).

[8] Hashia, B., Mir, A. H., "Segmentation techniques for the diagnosis of intervertebral disc diseases", Methods and Applications, 99–112, (2020).

[9] Han, Z., Wei, B., Mercado, A., Leung, S., Li, S., "Spine-GAN: Semantic segmentation of multiple spinal structures", Medical Image Analysis, 50: 23–35, (2018).

[10] Lessmann, N., Van Ginneken, B., de Jong, P. A., Išgum, I., "Iterative fully convolutional neural networks for automatic vertebra segmentation and identification", Medical Image Analysis, 53: 142–155, (2019).

[11] Simonovich, A., Nagar Osherov, A., Linov, L., amp; Kalichman, L. "The influence of knee bolster on lumbar spinal stenosis parameters on Mr Images, Skeletal Radiology, 49(2): 299–305, (2019).

[12] Lee, S., Lee, J. W., Yeom, J. S., Kim, K.J., Kim, H.-J., Chung, S. K., amp; Kang, H. S., "A practical MRI grading system for lumbar foraminal stenosis", American Journal of Roentgenology, 194(4): 1095–1098, (2010).

[13] Ronneberger, O., Fischer, P., Brox, T., "U-Net: Convolutional Networks for Biomedical Image Segmentation", Medical Image Computing and Computer-Assisted Intervention (MICCAI), Springer, LNCS, 234-241, (2015).

[14] Guo, Y., Duan, X., Wang, C., Guo, H., "Segmentation and recognition of breast ultrasound images based on an expanded U-Net", PLOS ONE, 16(6): e0253202, (2021).

[15] Ozturk, O., Saritürk, B., Seker, D. Z., "Comparison of Fully Convolutional Networks (FCN) and U-Net for Road Segmentation from High Resolution Imageries", International Journal of Environment and Geoinformatics, 7(3): 272–279, (2020).

[16] Zhao, W., Jiang, D., Peña Queralta, J., Westerlund, T., "MSS U-Net: 3D segmentation of kidneys and tumors from CT images with a multi-scale supervised U-Net", Informatics in Medicine Unlocked, 19, 100357, (2020).

[17] Shehab, L. H., Fahmy, O. M., Gasser, S. M., El-Mahallawy, M. S, "An efficient brain tumor image segmentation based on deep residual networks (ResNets)", Journal of King Saud University - Engineering Sciences, 33(6): 404–412, (2021).

[18] Lu, S., Wang, S. H., and Zhang, Y. D., "Detecting pathological brain via ResNet and randomized neural networks", Heliyon, 6(12): e05625, (2020).

[19] Dong, N., Zhao, L., Wu, C., Chang, J., "Inception v3 based cervical cell classification combined with artificially extracted features", Applied Soft Computing, 93: 106311, (2020).

[20] Zhang, Z., Wu, C., Coleman, S., and Kerr, D., "DENSE-INception U-net for medical image segmentation", Computer Methods and Programs in Biomedicine, 192: 105395, (2020).

[21] Pravitasari, A.A., Iriawan, N., Almuhayar, M., Azmi, T., Irhamah, I., Fithriasari, K., Purnami, S.W., Ferriastuti, W., "UNet -VGG16 with transfer learning for MRI-based brain tumor segmentation", TELKOMNIKA (Telecommunication Computing Electronics and Control), 18(3): 1310-1318, (2020).

[22] Ghosh, S., Chaki, A., Santosh, K., "Improved U-Net architecture with VGG-16 for brain tumor segmentation", Physical and Engineering Sciences in Medicine, 4(10), (2021).

[23] Alkan, A., "Analysis of knee osteoarthritis by using fuzzy c-means clustering and SVM classification", Scientific Research and Essays, 6(20): 4213-4219, (2011).

[24] Tuncer, A. S., "Spinal Cord Based Kidney Segmentation Using Connected Component Labeling and K-Means Clustering Algorithm", Traitement du Signal, 36(6): 521-527, (2019).

[25] Van der Graaf, J. W., Van Hooff, M. L., Buckens, C. F. M., Lessmann, N., "Segmentation of vertebrae and intervertebral discs in lumbar spine MR images with iterative instance segmentation", Medical Imaging 2022: Image Processing, (2022).

[26] Silvoster M.L., Mathusoothana, S., Kumar, R., "Efficient segmentation of lumbar intervertebral disc from MR images", IET Image Processing, 14(13): 3076–3083, (2020).

[27] Cheng, Y.K., Lin, C.L., Huang, Y.C., Chen, J.C., Lan, T.P., Lian, Z.Y., Chuang, C.H., "Automatic Segmentation of Specific Intervertebral Discs through a Two-Stage MultiResUNet Model", Journal of Clinical Medicine, 10(20): 4760, (2021).